arXiv:1405.4379v1 [cond-mat.stat-mech] 17 May 2014

Incommensurate Short-Range Order in $S = 1$ Triangular Lattice Ising Antiferromagnet

Yusuke Tomita[1,*] and Milan Žukovič[2]

[1] *College of Engineering, Shibaura Institute of Technology, Saitama 330-8570, Japan*
[2] *Department of Theoretical Physics and Astrophysics, Faculty of Science, P. J. Šafárik University, Park Angelinum 9,041 54 Košice, Slovakia*

(Dated: May 20, 2014)

We study the $S = 1$ triangular lattice Ising antiferromagnet by Monte Carlo simulations. Frustrations between a major antiferromagnetic third-neighbor interaction J_3 and a minor ferromagnetic nearest-neighbor interaction J_1 cause incommensurate short-range orders at intermediate temperatures. At low temperatures (below $T/J_3 \lesssim 0.2$ for $J_1/J_3 = -1/3$), the system exhibits fourfold periodic ordered state. In the short-range order phase, the system shows a glassy two-step relaxation. We demonstrate that the features of the short-range order are attributed to the cooperation between the frustrations and the nonmagnetic Ising spin states which is a particular feature of the integer spin systems.

Suppressed magnetic order in geometrically frustrated systems[1] has been attracting attention in material science and statistical physics. In particular, understanding disordered states solely by frustration (i.e., without randomness) has been an important challenge in both theoretical and experimental physics, because such disordered states can be qualitatively different from high-temperature paramagnetic states in terms of topological order[2–4] or pseudo-critical behavior[5]. A simplest frustrated spin model is the triangular lattice antiferromagnetic Ising model[6]. Strong frustration in the model suppresses the spontaneous emergence of order at finite temperatures. An extension of the model to the $S = 1$ Ising model[7] alleviates the frustration, and the extended model exhibits the Berezinskii-Kosterlitz-Thouless (BKT) transitions[8, 9]. Thus, in view of realizing a cooperative short-range order phase at finite temperature, frustration in the former model is too strong while it is too weak in the latter. In this Letter, we demonstrate that incommensurability introduced in the $S = 1$ model by adding the further-neighbor interaction can stabilize a peculiar short-range ordered phase with a glass-like *dynamical* property.

The Hamiltonian of the J_1-J_3 model is given by

$$\mathcal{H} = J_1 \sum_{\langle i,j \rangle} \sigma_i \sigma_j + J_3 \sum_{[i,k]} \sigma_i \sigma_k, \qquad (1)$$

where $\sigma_i (\in \{0, \pm 1\})$ represents an $S = 1$ Ising spin at site i. In the right hand side of Eq. (1), the first term represents the ferromagnetic nearest-neighbor interactions ($J_1 < 0$), and the second term represents the antiferromagnetic third-neighbor interactions ($J_3 > 0$). For $J_1 = 0$, the model comprises four decoupled sublattices of the $S = 1$ triangular lattice Ising model. Unlike the $S = 1/2$ triangular lattice Ising antiferromagnetic system, the antiferromagnetic interactions give rise to the BKT transitions at finite temperatures[7, 10]. The BKT transition of the model is described by the Z_6 symmetry breaking corresponding to the three-sublattice structure $(+1, 0, -1)$: Since the triangular lattice is a tripartite lattice, each of the three states of the $S = 1$ Ising spin can avoid neighboring the same state. Such favorable states in energetical point of view degenerate into six states. The ordered state is almost the same as the 120° structure in the six-state antiferromagnetic clock model on the triangular lattice, but there are inhomogeneities in energies at sites. By introducing a small nearest-neighbor ferromagnetic coupling J_1, the four triangular sublattices are coupled, leading to a different ground state. Here, we note that $|J_1| \ll J_3$ is not necessarily an unrealistic assumption. Such a situation can be realized when the system possesses some combination of direct and superexchange couplings as in a $S = 1$ quantum antiferromagnet $NiGa_2S_4$. Below we set $J_1/J_3 = -1/3$ corresponding to an estimate in this compound[11]. By analyzing the Fourier transform of the exchange couplings, we find that a magnetic instability may occur at incommensurate (IC) wave vectors $\pm(k, 0)$, $\pm(k/2, \sqrt{3}k/2)$, and $\pm(k/2, -\sqrt{3}k/2)$ for $-4 < J_1/J_3 < 0$, where k is determined by[12]

$$J_1/J_3 = -[2(\sin k + \sin 2k)]/[\sin k + \sin(k/2)]. \qquad (2)$$

Using Eq. (2), we obtained $k \simeq 1.922$ for $J_1/J_3 = -1/3$.

To investigate thermal equilibrium properties of the J_1-J_3 model, Monte Carlo (MC) simulations are executed. The Suwa-Todo algorithm[13] that minimizes the average of rejection rate is employed to improve spin updates. The triangular lattice of the system size L contains $N(= L^2)$ spins, and the periodic boundary conditions are imposed. To estimate thermal averages, $N_{\rm MCS} = 2 \times 10^7$ (1×10^7) MC steps are executed for $L = 144$, 192, and 288 ($L = 48$, 72, and 96). The simulations start from the highest temperature ($T/J_3 = 1.1$), and the temperature is gradually lowered with the step $\Delta T/J_3 = 0.01$. For thermalization at each temperature, $0.2 \times N_{\rm MCS}$ MC steps are discarded before measuring observables. To estimate statistical errors, independent 10 samples are simulated. Hereafter, Boltzmann constant $k_{\rm B}$ is set to unity.

Figures 1 show the internal energy and specific heat per site for several system sizes. We observed the spe-

cific heat jump at $T/J_3 \sim 0.2$ for $L = 192$ and 288 (data are not shown for the visibility). Scatterings of the specific heat data are observed in $0.2 \lesssim T/J_3 \lesssim 0.9$. To analyze the origin of the data scattering, we calculate the structure factor,

$$S(\boldsymbol{k}) = \langle \sigma_{\boldsymbol{k}} \sigma_{-\boldsymbol{k}} \rangle, \tag{3}$$

where $\sigma_{\boldsymbol{k}}$ denotes the Fourier transform of the spins and $\boldsymbol{k}$ is the wavevector.

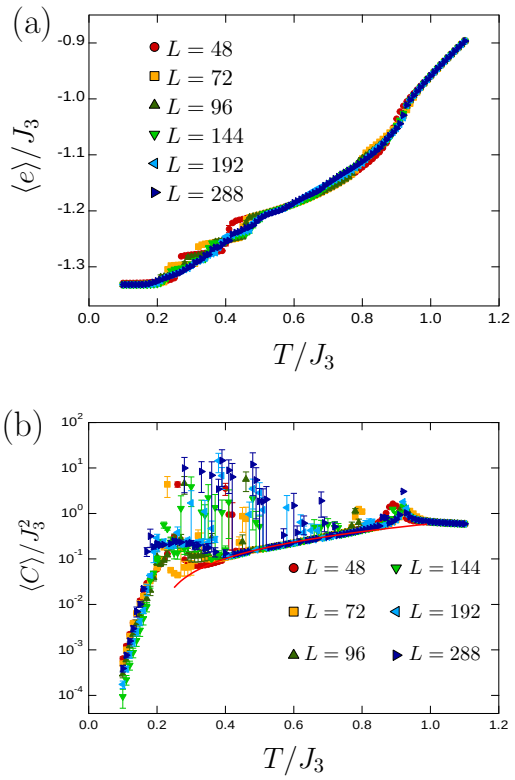

FIG. 1. (Color online) (a) Plot of the internal energy per site. Error bars are smaller than size of marks. (b) Semi-logarithmic plot of the specific heat. The solid curve is a quadratic curve that fits the intermediate data. Since the specific heat jump at $T/J_3 \sim 0.2$ is extremely large (10^5 order) for $L = 192$ and 288, they are omitted for the visibility.

Structure factors for $L = 192$ are plotted in Figs. 2(a)-2(c). The structure factor at $T/J_3 = 0.7$ shows six peaks. The positions of the peaks are the same positions given by Eq. (2) within the accuracy of the lattice discreteness. This coincidence is explained by the universality class of the six-state clock model. The clock model has two transition points, and the universality class of the transition point at the higher temperature is the same as the XY model. Since thermal fluctuations screen the discreteness of the clock model, the system exhibits the universality class of the XY model. In the J_1-J_3 model, each triangle of Ising spins behaves like a planer spin variable[7, 10] around $T/J_3 = 0.7$, so that the structure factor exhibits the development of the spin-spin correlations same as the continuous spins. Hereafter we call the magnetic short-range order (SRO) as the planer order.

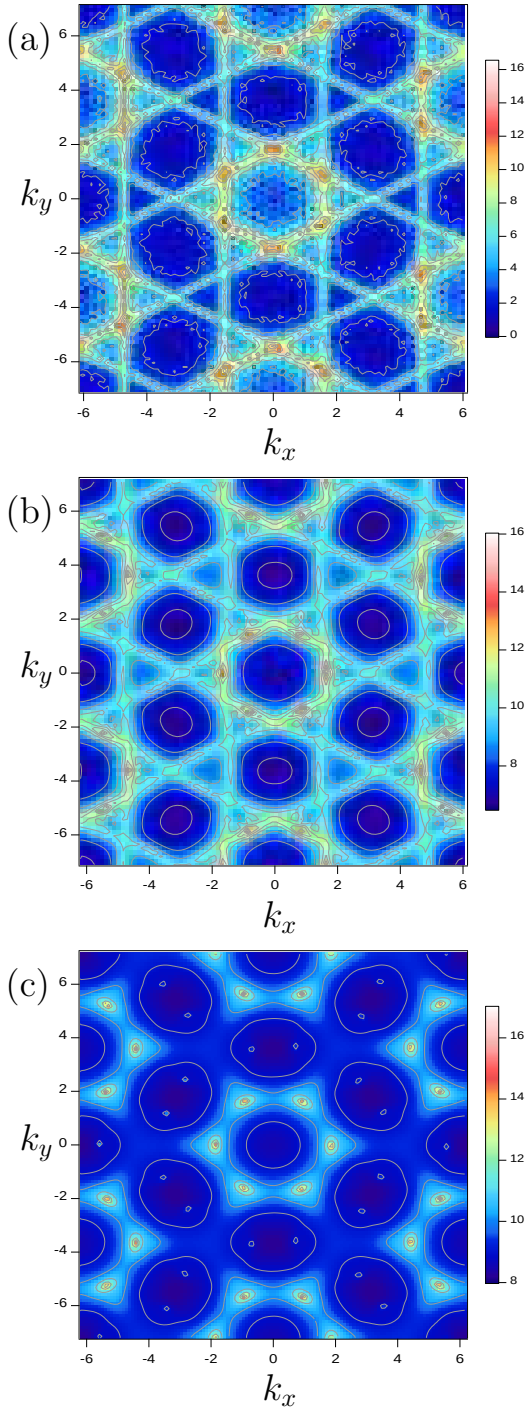

FIG. 2. (Color online) Structure factors for $L = 192$ at three different temperatures are plotted. Temperatures of the plots are (a) $T/J_3 = 0.15$, (b) $T/J_3 = 0.3$, and (c) $T/J_3 = 0.7$. To improve visualization, the natural logarithmic scale is adopted for structure factors. Contour lines are superimposed.

The opposite situation arises at low temperatures ($T/J_3 \lesssim 0.2$). In the low temperatures, thermal fluc-

tuations are too weak to screen the discreteness of spin variables, and an ordered state resulting from the discreteness of the Ising spin emerges. The ordered state is a fourfold periodic spin configuration (↑↑↓↓). Hereafter we call the magnetic structure as the low-T order. Since spin configurations obtained by MC simulations consist of domains of the fourfold periodic pattern, six peaks are observed at $\pm(0,\ \pi/\sqrt{3})$, $\pm(\pi/2,\ \pi/(2\sqrt{3}))$, and $\pm(\pi/2,\ -\pi/(2\sqrt{3}))$ in the structure factor. The perfect fourfold structure gives the internal energy per site $\langle e\rangle/J_3 = -4/3$, whereas internal energies obtained by the MC simulations are slightly higher than $-4/3$.

In a rather wide window of the intermediate temperatures ($0.2 \lesssim T/J_3 \lesssim 0.9$), the peaks in the structure factor become less sharp (i.e., the correlation length decreases) as lowering the temperature, while the peak positions remain almost the same as those at $T/J_3 = 0.7$. In Fig. 3, we show the correlation length defined by

$$\xi = \frac{1}{2\sin(\Delta k/2)}\sqrt{\frac{S(k_{\max})}{S(k'_{\max})} - 1}, \tag{4}$$

where $\Delta k = 2\pi/L$ and $S(k_{\max})$ and $S(k'_{\max})$ are, respectively, the structure factor averaged at six peaks and that averaged at neighboring sites of the peaks. At least according to snapshots of the spin configuration (not shown), the temperature dependence of the magnetic domain is as follows: Planer SRO domains adjoin each other at rather high temperatures ($0.5 \lesssim T/J_3 \lesssim 0.9$), while the domains are separated by thick domain walls at lower temperature. At rather low temperatures ($0.2 \lesssim T/J_3 \lesssim 0.5$), domain walls become thicker as the temperature is lowered. The low-T order appears in the thick domain walls, and it becomes the dominant order at $T/J_3 \sim 0.2$.

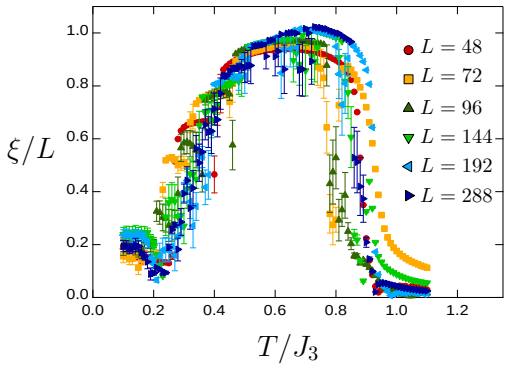

FIG. 3. (Color online) Plot of the normalized correlation length ξ/L for several system sizes.

The competition between the planer IC order and the low-T fourfold periodic order reminds us the modulated and floating IC phase in the axial next-nearest neighbor Ising (ANNNI) model[14]. The modulated phase consists of a lot of periodic phases, and each phase is separated by the first-order transition. Though the magnetic structure in the J_1-J_3 model is incommensurate, there might be temperatures that the IC magnetic patterns approximately match the lattice spacing. At such temperatures, energy fluctuations become larger, and data scattering in the specific heat is observed.

If the above analogy between the J_1-J_3 model and the ANNNI model is appropriate, the magnetic domains exhibit unusual relaxation process. The most distinguished dynamical feature of the ANNNI model is the floating IC phase, in which floating (not locked) domain walls are observed. To investigate the dynamical feature of the J_1-J_3 model, we calculated a time-displaced correlation function,

$$\psi(t) = \frac{\langle \sum_i^N \sigma_i(t)\sigma_i(0)\rangle}{\langle \sum_i^N \sigma_i^2(0)\rangle}, \tag{5}$$

where $\langle\cdots\rangle$ denotes the thermal average. Since this quantity is affected by spin update methods, we changed the method from the Suwa-Todo algorithm to the heat bath method. In Fig. 4, we plot the correlation functions. The correlation function shows exponential decays in paramagnetic phase ($T/J_3 = 1.0$), whereas the correlations in the planer IC phase ($T/J_3 = 0.6$ and 0.3) gradually decay in time. Oscillating behavior in ψ's in the planer IC phase indicates that domains are floating, since displaced domains make ψ negative. Qualitative differences in relaxations of the correlation function between that of $T/J_3 = 0.6$ and of $T/J_3 = 0.3$ are quite interesting. At the first stage ($t \lesssim 10$), ψ's at $T/J_3 = 0.6$ show fast decays, while ψ's at $T/J_3 = 0.3$ show monotonic decays. The fast decay is probably attributed to relaxations around nonmagnetic states ($\sigma = 0$). Since interaction energies around nonmagnetic states are zero regardless of their spin states, relaxations should be faster than those around magnetic states. The heterogeneities in the energy and dynamics remind us of the rattling motion in glassy materials[15–17]. The nonmagnetic states give rise to *cage structures* as in glass formers and kinetically constrained models[18–20]. As the temperature is lowered, correlations of the low-T order are enhanced, so that the density of nonmagnetic spins at $T/J_3 = 0.3$ is not sufficient enough to show the rattling motion. At the second stage ($10 \lesssim t \lesssim 10^3$), ψ's at $T/J_3 = 0.6$ show quite slow relaxation; slopes are flatter than those at $T/J_3 = 0.3$. This slow relaxation is explained by the crossover from the BKT phase. As we mentioned above, each triangle of Ising spins is regarded as planer spin variable when thermal fluctuations are sufficiently strong. Considering that the peak positions of the structure factor in the planer SRO phase are located near those of planer spin systems, the triple Ising spins are behaving like planer spins. In addition, the sharpness of the peaks indicates that systems at higher temperatures are more likely to be affected by the BKT phase. The plateau regime observed

at $T/J_3 = 0.6$ is similar to the β-relaxation in glassy materials. To the best of our knowledge, the mechanism of the emergence of the β-relaxation in glassy materials has not been unveiled. However, in the J_1-J_3 model, the emergence of the plateau regime can be interpreted as the crossover from the BKT phase.

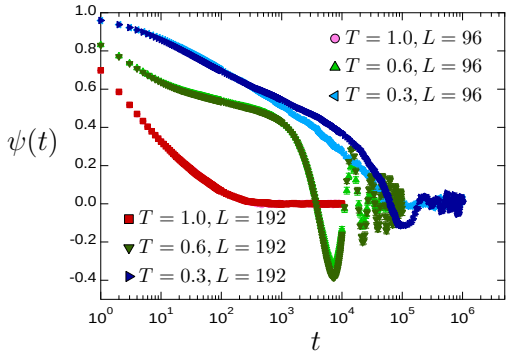

FIG. 4. (Color online) Plot of the time-displaced correlation function for $L = 96$ and $L = 192$ at three different temperatures.

One might be interested in constructing a spin model which exhibits no long-range order at finite temperatures. Such a spin model is probably realized by introducing chemical potential term $\mu \sum_i \sigma_i^2$ into the J_1-J_3 model. By setting the parameter μ sufficiently positively large, the planer SRO phase pushes out the low-T order phase.

Albeit many differences, thermal properties of the Ising J_1-J_3 model are surprisingly quite similar to those of $NiGa_2S_4$[11] at least at a phenomenological level. Though our model has the low-T order phase, the ordered phase is probably eliminated by introducing the chemical potential term as mentioned above. By including such a chemical potential term, the J_1-J_3 model would exhibit no long-range order at finite temperatures, which is consistent with the observation in $NiGa_2S_4$ at least phenomenologically. Dynamics of the J_1-J_3 model also have similarities to $NiGa_2S_4$. As shown in Fig. 4, the J_1-J_3 model exhibits quasi-critical relaxation in the planer SRO phase. Since the quasi-critical relaxation originates from the crossover from the BKT transition, planer SRO states at higher temperatures are more affected by the crossover. The dynamical crossover in the J_1-J_3 model is similar to the signal lost in Ga-nuclear quadrupole resonance[21] and the non-monotonic linewidth growth in electron spin resonance[22].

There are two grounds for the similarities. The first one is that the J_1-J_3 model possesses the emergent planer spin symmetry in the planer SRO phase, which might be related to the easy-plane anisotropy of the $S = 1$ Heisenberg spins in $NiGa_2S_4$[23]. The other similarity is the one between $S = 1$ Ising and quantum Heisenberg spins in a sense that the Hilbert space is identical. The discreteness of the Ising spin is consistent with the discreteness of the quantum spin state. A notorious deficiency of classical Heisenberg spin systems is that they estimate the specific heat at unity in the limit of $T = 0$. Therefore, classical continuous spin systems are not suitable for studying of quantum spin systems at low temperatures. Moreover, the $S = 1$ Ising spin emulates the nonmagnetic state ($\sigma = 0$) in quantum spin systems. The classical Heisenberg spin does not have this feature, and the lack of the feature causes the long-range order at low temperatures[12, 24]. Even though the $S = 1$ quantum Heisenberg J_1-J_3 model exhibits an antiferromagnetic long-range order when $J_1/J_3 = -1/3$, short-range order emerges in the range of $-4.0 \lesssim J_1/J_3 \lesssim -2.2$[25]. The importance of the feature has already been pointed out by one of the authors in the study of variable-length Heisenberg spin model[26]. The significant influence by nonmagnetic states is also consistent with experimental observations. Nambu and Nakatsuji studied the spin-size dependent impurity effects by $Ni_{1-x}A_xGa_2S_4$ [A = Zn ($S = 0$), Fe ($S = 2$), Co ($S = 3/2$), and Mn ($S = 5/2$)][27]. They found that the integer spin impurities do not bring about a drastic change, whereas the canonical spin glass-like behavior is observed with the substitution of the magnetic impurities with half-odd integer spins. Understanding the difference between integer and half-integer spins is easy if the analogy between the $S = 1$ Ising J_1-J_3 model and $NiGa_2S_4$ is applicable. Due to pinning of floating planer IC domains at half-integer spin impurity sites, the *floating* IC phase is taken over by the *randomly locked* IC phase. On the other hand, integer spin impurities are not able to pin a floating domain, so that no significant change emerges. Though the symmetry of the Ising spin is different from the Heisenberg spin, the Ising spin system seems to be more suitable for describing the low temperature properties of $NiGa_2S_4$ than the classical Heisenberg spin models.

Conclusions.— We have performed MC simulations of the 2D $S = 1$ Ising J_1-J_3 model. The model exhibits three phases; the paramagnetic, the intermediate planer SRO, and the fourfold periodic ordered phase. In the planer SRO phase, the true long-range order is absent, since magnetic domains are floating. However, the time-displaced correlation function shows quasi-critical relaxation, because of the crossover from the BKT transition. The two-step relaxation process observed at higher temperatures is quite similar to the relaxation process in glass formers. Quite interestingly, the relaxation process is emerged from purely geometric frustration in the simple spin model. We expect that our model provides a good foothold for understanding slow dynamics in frustrated and/or glassy systems. While the symmetry of our spin model is different from that of $NiGa_2S_4$, because of the identical structure of the Hilbert space, we show that our spin model can phenomenologically reproduce several aspects observed in $NiGa_2S_4$. Even though our model is

not the exact model of $NiGa_2S_4$, studying the model will help to understand frustrated magnets.

We thank Y. Kamiya for valuable discussions and useful comments on the manuscript. The computation in the present work was performed on computers at the Supercomputer Center, Institute for Solid State Physics, University of Tokyo.

* ytomita@shibaura-it.ac.jp

[1] A. P. Ramirez, Annu. Rev. Mater. Sci. **24**, 453 (1994).
[2] X. G. Wen, Int. J. Mod. Phys. **B4**, 239 (1990).
[3] A. Kitaev, Ann. Phys. (N. Y.) **321**, 2 (2006).
[4] S. V. Isakov, M. B. Hastings, and R. G. Melko, Nat. Phys. **7**, 772 (2011).
[5] S.-Z. Lin, Y. Kamiya, G.-W. Chern, and C. D. Batista, Phys. Rev. Lett. **112**, 155702 (2014).
[6] G. H. Wannier, Phys. Rev. **79**, 357 (1950).
[7] M. Žukovič and A. Bobák, Phys. Rev. E **87**, 032121 (2013).
[8] V. L. Berezinskii, Sov. Phys. JETP **32**, 493 (1971).
[9] J. M. Kosterlitz and D. J. Thouless, J. Phys. C **6**, 1181 (1973).
[10] D. P. Landau, Phys. Rev. B **27**, 5604 (1983).
[11] S. Nakatsuji, Y. Nambu, H. Tonomura, O. Sakai, S. Jonas, C. Broholm, H. Tsunetsugu, Y. Qiu, and Y. Maeno, Science **309**, 1697 (2005).
[12] R. Tamura and N. Kawashima, J. Phys. Soc. Jpn. **77**, 103002 (2008); **80**, 074008 (2011).
[13] H. Suwa and S. Todo, Phys. Rev. Lett. **105**, 120603 (2010).
[14] W. Selke, Phys. Rep. **170**, 213 (1988).
[15] T. Muranaka and Y. Hiwatari, Phys. Rev. E **51**, R2735 (1995).
[16] W. Kob, C. Donati, S. J. Plimpton, P. H. Poole, and S. C. Glotzer, Phys. Rev. Lett. **79**, 2827 (1997).
[17] E. R. Weeks, J. C. Crocker, A. C. Levitt, A. Schofield, and D. A. Weitz, Science **287**, 627 (2000).
[18] G. H. Fredrickson and H. C. Andersen, Phys. Rev. Lett. **53**, 1244 (1984).
[19] W. Kob and H. C. Andersen, Phys. Rev. E **48**, 4364 (1993).
[20] G. Biroli and M. Mézard, Phys. Rev. Lett. **88**, 025501 (2001).
[21] H. Takeya, K. Ishida, K. Kitagawa, Y. Ihara, K. Onuma, Y. Maeno, Y. Nambu, S. Nakatsuji, D. E. MacLaughlin, A. Koda, and R. Kadono, Phys. Rev. B **77**, 054429 (2008).
[22] H. Yamaguchi, S. Kimura, M. Hagiwara, Y. Nambu, S. Nakatsuji, Y. Maeno, and K. Kindo, Phy. Rev. B **78**, 180404 (2008).
[23] H. Yamaguchi, S. Kimura, M. Hagiwara, Y. Nambu, S. Nakatsuji, Y. Maeno, A. Matsuo, and K. Kindo, J. Phys. Soc. Jpn. **79**, 054710 (2010).
[24] E. M. Stoudenmire, S. Trebst, and L. Balents, Phys. Rev. B **79**, 214436 (2009).
[25] P. Rubin, A. Sherman, and M. Schreiber, Phys. Lett. A **376**, 1062 (2012).
[26] Y. Tomita and N. Kawashima, J. Phys. Soc. Jpn. **80**, 054001 (2011).
[27] Y. Nambu, S. Nakatsuji, Y. Maeno, E. K. Okudzeto, and J. Y. Chan, Phys. Rev. Lett. **101**, 207204 (2008); Y. Nambu and S. Nakatsuji, J. Phys.: Condens. Matter **23**, 164202 (2011).